Periodic lattice distortion accompanying the (3×3) charge-density-wave phase of Sn/Ge(111)

A. P. Baddorf and V. Jahns
Solid State Division, Oak Ridge National Laboratory, Oak Ridge, Tennessee 37831-6030

Jiandi Zhang, J. M. Carpinelli, and E. W. Plummer
Solid State Division, Oak Ridge National Laboratory, Oak Ridge, Tennessee 37831-6030
and Department of Physics and Astronomy, The University of Tennessee, Knoxville, Tennessee 37996-1200
(Received 10 November 1997)

Surface x-ray diffraction has been used to determine the periodic lattice distortion (PLD) accompanying the charge-density-wave (CDW) formation in the α phase of Sn on Ge(111). Scanning tunneling microscopy observations of the CDW show a $\sim$0.5-Å vertical charge corrugation in the image of the Sn atoms, but the measured vertical ripple in the PLD is almost zero, $\sim 0.04\pm 0.04$ Å. The PLD occurs almost exclusively in the outermost Ge layer, where a 0.22-Å lateral motion of the three Ge atoms is associated with the Sn atom with largest amplitude in the CDW. Surprisingly, Sn ion cores move in the opposite direction from valence electrons. These results will be discussed in light of the recent models put forward to explain the CDW formation. [S0163-1829(98)01708-1]

The α phase ($\frac{1}{3}$ of a monolayer) of both Pb (Refs. 1 and 2) and Sn (Refs. 3 and 4) overlayers on Ge(111) show a dramatic charge ordering transition in scanning tunneling microscope (STM) images as the temperature is lowered.[5,6] Low-energy electron diffraction (LEED) images show that, as expected, there is a periodic lattice distortion (PLD) that accompanies this charge-density wave (CDW). The PLD results in a transition from Ge(111)-$(\sqrt{3}\times\sqrt{3})R30°$-$x$ to a commensurate Ge(111)-(3×3)-x (x is Pb or Sn) structure,[5,6] the details of which are unknown. For the Pb system, density-functional calculations by Carpinelli *et al.*[5] indicate that the PLD lowers the total energy of the system, while for the isoelectronic Sn overlayer a PLD is unstable.[6] Experimentally, the CDW phase of Pb is nonmetallic,[5,7] indicating that electron correlation stabilizes the PLD, while the Sn overlayer is metallic in the CDW phase.[6] Recent photoemission measurements by Goldoni and Modesti[8] show a dramatic change in the Sn-induced bands as the CDW forms, indicating (according to the authors) strong correlation effects in the Sn CDW. Finally, the photoemission measurements on the Sn system[8] coupled with response function calculations from the calculated Fermi contour[6] clearly show that Fermi-surface nesting is not the driving force for the CDW formation in Sn, as was speculated for the Pb system.[5]

The origin of the CDW in both systems is at present unknown. The structure associated with the PLD will be crucial information for any physical explanation, yet the STM images have shed no light on the nature of the PLD. In fact, an average of empty- and filled-state images of the low-temperature phase approximates the image of the uniform room-temperature phase, implying the CDW need not involve any atomic displacement of the Sn.[6] On the other hand, arguments based upon the relative intensity of the (3×3) fractional-order beams in the LEED pattern compared to the integral-order beams point to a lattice distortion of the order of at least 0.1 Å.[9] We have utilized the technique of surface x-ray diffraction[10] (XRD) to address the important issue of the magnitude and character of the lattice distortion that accompanies the CDW. The data indicate that the PLD is confined almost entirely to the Sn and first Ge layer, i.e., no deep reconstruction. Surprisingly, there is little distortion of the Sn atoms induced by the CDW, but three of the nine Ge atoms in the surface plane in the new (3×3) unit cell move laterally 0.22 Å further towards the Sn atom that, according to STM, has an excess of filled states. We will argue that this large distortion places this CDW in the category of a ''strong-coupling CDW'' (terminology introduced by Tosatti[11]), in contrast to a ''weak-coupling CDW'' as indicated by the calculations of Carpinelli *et al.*[5] for the Pb system.

Surface x-ray diffraction has been utilized because it has greater sensitivity to deeper lattice distortions than does LEED and involves only kinematic scattering.[10] Kinematic scattering makes analysis significantly easier, considering the large number of atoms in the two-dimensional unit cell, and allows specific components of displacement to be isolated (along the direction of momentum transfer), which is not possible when multiple scattering is significant. The structure of the low-temperature Ge(111)-(3×3)-Sn interface was determined by fitting data for 13 independent diffraction rods, and compared to the α phase room-temperature Ge(111)-$(\sqrt{3}\times\sqrt{3})R30°$-Sn structure determined from 12 independent rods.

Clean, well-ordered Ge(111) surfaces were prepared in ultrahigh vacuum by repeated Ar ion bombardment and annealing to $T=925$ K until a sharp $c(2\times8)$ LEED pattern was observed. Sn was deposited at room temperature from a Knudson cell that had previously been calibrated with Auger electron spectroscopy and STM investigations.[6] After deposition of $\sim\frac{1}{3}$ of a monolayer of Sn, the surface was annealed to 500 K. Annealing resulted in the formation of a sharp $(\sqrt{3}\times\sqrt{3})R30°$ overlayer observed with LEED. Diffraction spots from the new (3×3) unit cell associated with the CDW appeared in LEED when the sample was cooled. Both (3×3) and $(\sqrt{3}\times\sqrt{3})R30°$ LEED patterns exhibit C_{3v} symmetry, a symmetry originating with the bulk Ge(111)

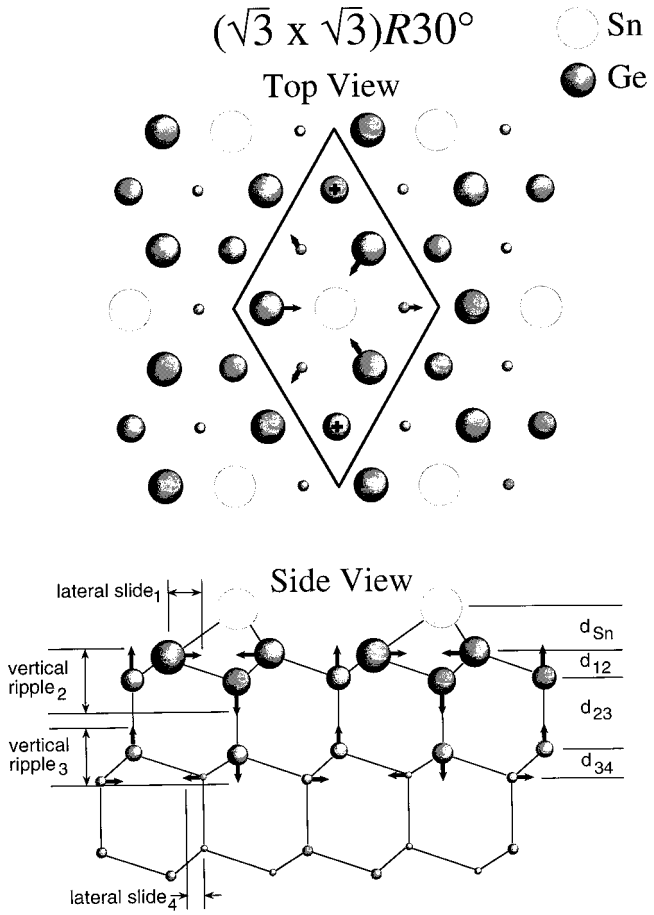

FIG. 1. Structural model of Ge(111)-$(\sqrt{3}\times\sqrt{3})R30°$-Sn. The top is a view from above the surface and the bottom is a side view. Ge atoms are drawn in bulk-truncated positions, with arrows to show the direction of distortions induced by Sn; plus signs indicate motion out of the plane of the figure. Arrow lengths are not to scale.

planes.[6] The transition was observed to be gradual and reversible with a critical temperature $T_c \sim 215$ K, compared to the value of 255 K for the Pb system.[4] X-ray diffraction measurements were made on beam line x-2A at the National Synchrotron Light Source using a z-axis geometry diffractometer and scattering chamber. Diffraction intensities of 10.5 keV x rays were measured by integrating transverse scans across surface rods using procedures and analysis described previously.[10,12] Reference surface diffraction intensities were monitored and new surfaces prepared before changes exceeded $\sim$30%, which allowed scans for up to 12 h at 1×10^{-10} Torr. To promote surface sensitivity, a logarithmic scale was used to compare calculations from test models with measured intensities, which is also how they are most commonly displayed. Quality of fits are expressed both as R-factor values, R_2,[13] and as reduced χ^2 values.

Figure 1 shows a ball model of the Ge(111)-$(\sqrt{3}\times\sqrt{3})R30°$-Sn structure. The bottom picture is a side view showing the Sn overlayer and three bilayers of Ge. Both of these diagrams show Ge atoms in the bulk positions associated with a (1×1) LEED pattern. The arrows indicate the direction of the distortion of Ge atoms induced by the presence of Sn atoms on the surface. Structural parameter values are give in Table I. The extended range of momentum transfer in this study compared to the earlier XRD study of Pedersen *et al.*[4] resulted in a significantly different structure for room-temperature Ge(111)-$(\sqrt{3}\times\sqrt{3})R30°$-Sn. Both studies indicate a deep distortion of the Ge atoms caused by the presence of Sn, but in contrast to the Pedersen *et al.*[4] structure our analysis has a very small lateral slide in the first Ge bilayer. In addition, the distance of the Sn from the first Ge layer is significantly larger for our structural model (1.91 Å compared to 1.72 Å). A discussion of the differences and their basis will be left for a future publication. The important observation is that the formation of the Ge(111)-$(\sqrt{3}\times\sqrt{3})R30°$-Sn structure results in deep but primarily vertical distortions of the Ge substrate. There is almost no distortion of the first Ge layer (only a 0.05 Å lateral motion of the Ge towards the Sn). This is an important observation, since, as we will show, the PLD accompanying the CDW formation is a large lateral motion of the Ge surface atoms.

When the room-temperature Ge(111)-$(\sqrt{3}\times\sqrt{3})R30°$-Sn phase is cooled below $\sim$215 K, sharp (3×3) diffraction spots appear in the observed LEED pattern. With the high-momentum resolution available with XRD it is seen that the PLD in the CDW phase is indeed commensurate with the substrate. Peak positions from an ensemble of transverse scans across the nominal $(\frac{2}{3},0)$ rod yield an experimental position of $(0.6694\pm0.007,\ -0.0058\pm0.015)$ which is within error equal to the nominal value.

Figure 2 displays the x-ray diffraction data for the low-temperature (3×3) structure for 13 different rods acquired at 90 K. The left-hand panel shows bulk truncation rods and the right-hand panel displays diffraction rods associated with the Sn-induced restructuring of the surface. Only one rod in the collected data, the $(\frac{2}{3},0)$, is uniquely associated with the (3×3) structure; all of the other surface rods are common with both the $(\sqrt{3}\times\sqrt{3})R30°$ and the (3×3) structure. In each panel, the top rod is plotted as an absolute intensity per incident photon. Rods beneath have been offset by dividing by a factor of 10 between each curve, with the exception of the $(2,-1)$ and $(1,0)$ rods in the left panel, which are offset by a factor of 100. The best fits to the data are shown as a solid line in Fig. 2 and corresponding parameter values are listed in column 3 of Table I.

Surprisingly little difference, outside of Debye-Waller thermal effects, are observed in the x-ray diffraction after cooling. Visually, rods appearing at both temperatures have the same shape. New diffraction rods, such at the $(\frac{2}{3},0)$ rod shown in Fig. 2, are extremely weak. Compared to the $(\frac{2}{3},-\frac{1}{3})$ rod, which has nearly the same magnitude of momentum transfer, the $(\frac{2}{3},0)$ rod has about $100\times$ smaller intensity. Low intensity made experimental measurements difficult; even after maximizing the surface sensitivity by using a grazing incidence geometry each data point along the $(\frac{2}{3},0)$ rod required 5–6 h of data collection.

The similarities in rod intensities shared by $(\sqrt{3}\times\sqrt{3})R30°$ and (3×3) phases indicate the two structures are closely related. To illustrate the small changes in the x-ray diffraction data we have compared the structure determined from the room-temperature data to the low-temperature data. The best fit to the low-temperature data produced a χ^2 of 1.08, with an R factor of 0.66% (column 3 of Table I). If one uses the low-temperature structure, fixing

TABLE I. Comparison of our structural determination (column 1) for Ge(111)-($\sqrt{3}\times\sqrt{3}$)$R30°$-Sn with the previous results of Pedersen *et al.* (Ref. 4) (column 2). Column 3 lists structural parameters for the low-temperature Ge(111)-(3×3)-Sn. Values are given with respect to bulk-truncated atomic positions. Numeric subscripts identify the pertinent layer. Parameters d indicate a layer spacing and Δd a deviation from the bulk spacings (0.82 Å within a bilayer and 2.45 Å between bilayers) measured from the midpoint position of atoms within the layer. Peak-to-peak values are presented for vertical ripples. In the (3×3) structure, two Sn atoms per unit cell and the neighboring Ge (A) are different from the third and its neighbors (B). See Fig. 1 for further parameter clarification. Uncertainties are based on a statistical analysis and represent $\pm\sigma$, assuming normally distributed errors.

Parameter	This study ($\sqrt{3}\times\sqrt{3}$)$R30°$ (Å)	Pedersen *et al.* ($\sqrt{3}\times\sqrt{3}$)$R30°$	This study (3×3)
	Structural parameters		
d_{Sn} (A)	1.91±0.20 Å	1.72 Å	1.85±0.22 Å
d_{Sn} (B)			1.81±0.22 Å
vertical ripple Sn			0.04±0.04 Å
lateral slide$_1$ (A)	0.05±0.02 Å	0.204 Å	0.04±0.02 Å
lateral slide$_1$ (B)			0.27±0.02 Å
vertical ripple$_2$ (A)	0.61±0.04 Å	0.58 Å	0.43±0.09 Å
vertical ripple$_2$ (B)			0.37±0.09 Å
vertical ripple$_3$	0.40±0.04 Å	0.58 Å	0.33±0.03 Å
lateral slide$_4$	0.04±0.02 Å	0.106 Å	0.03±0.02 Å
Δd_{12}	0.09±0.10 Å	−0.15Å	0.01±0.10 Å
Δd_{23}	−0.07±0.05 Å	0.00 Å	−0.07±0.10 Å
Δd_{34}	0.02±0.03 Å	0.41 Å	−0.02±0.02 Å
Δd_{45}	0.05±0.02 Å	0.00 Å	0.02±0.02 Å
	Thermal properties		
RMS Sn(z)	0.28±0.04 Å	0.195 Å	0.28±0.04 Å
RMS Sn(xy)	0.32±0.04 Å	0.195 Å	0.26±0.04 Å
RMS Ge$_1$(z)	0.20±0.05 Å	0.087 Å	0.17±0.03 Å
RMS Ge$_1$(xy)	0.16±0.04 Å	0.087 Å	0.15±0.04 Å
RMS Ge$_2$(z)	0.09±0.06 Å	0.087 Å	0.04±0.05 Å
RMS Ge$_2$(xy)	0.18±0.04 Å	0.087 Å	0.11±0.04 Å
RMS Ge$_3$(z)	0.25±0.05 Å	0.087 Å	0.07±0.05 Å
RMS Ge$_3$(xy)	0.09±0.04 Å	0.087 Å	0.09±0.04 Å
RMS Ge$_4$(z)	0.23±0.05 Å	0.087 Å	0.032 Å
RMS Ge$_4$(xy)	0.09±0.03 Å	0.087 Å	0.032 Å
RMS bulk	0.084 Å	0.086 Å	0.032 Å
	Quality of fit		
χ^2	1.9	8.7	1.08
R	1.2%	5.5%	0.66%

the structural parameters but allowing the vibrational parameters to vary, to fit the room-temperature data one obtains $\chi^2=2.65$ with an R factor of 1.86%. If then the positions of the Sn and outermost Ge layer ($\frac{1}{2}$ bilayer) are also optimized, the χ^2 drops to 2.2 and the R factor to 1.57%. If all the parameters are optimized, the best fit for the room-temperature structure is obtained (values in column 1 of Table I) with χ^2 of 1.9 and an R factor of 1.20%. The relatively low values of χ^2 and the R factor after optimization of only the Sn and outermost Ge layer lead us to conclude that the lattice distortion responsible for the (3×3) structure is primarily displacement of the Sn atoms and Ge atoms in the first plane.

The fundamental difference between the PLD accompanying the CDW and the reconstruction associated with the room-temperature phase is shown in Fig. 3, where experimental intensities for the ($\frac{2}{3}$,0) rod are compared to calculations for out-of and in-plane displacements of the Sn and first Ge layer. The physics is quite simple: if the distortion that causes the (3×3) structure is only vertical, then there is no intensity in this in-plane diffraction rod at $q_z=0$. The large intensity at $q_z=0$ is a consequence of a lateral distortion. This could be a displacement of Sn atoms; in fact a slide of two Sn atoms per unit cell by 0.2 Å leads to a χ^2 value of 1.21. A better physical picture and a lower χ^2 value (1.08) are obtained, however, with a lateral displacement of Ge atoms, which have already shown an inclination to move laterally (although much less) in the ($\sqrt{3}\times\sqrt{3}$)$R30°$ phase.

The best (3×3) structural model, with parameters shown in the third column of Table I, was obtained after R-factor comparison to the entire data set of Fig. 2. We restricted models to those consistent with evidence from STM images, where two atoms per unit cell appear identical, but different from the third, and from LEED, where C_{3v} symmetry is observed. The inset in Fig. 3 shows a ball model illustrating the dominant displacements that create the (3×3) PLD.

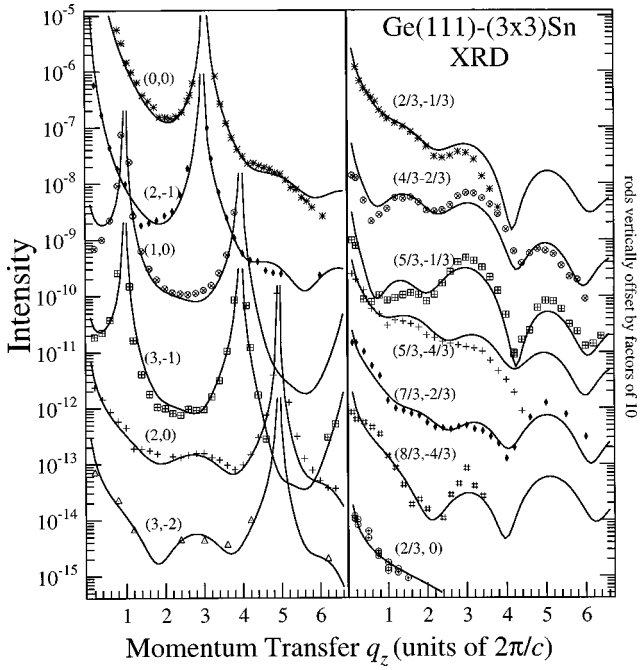

FIG. 2. X-ray diffraction rods for Ge(111)-(3×3)-Sn at $T = 90$ K. The solid line is the calculated diffraction intensity for the best-fit model. The periodic length normal to the surface, c, is 9.80 Å. Curves are offset for clarity.

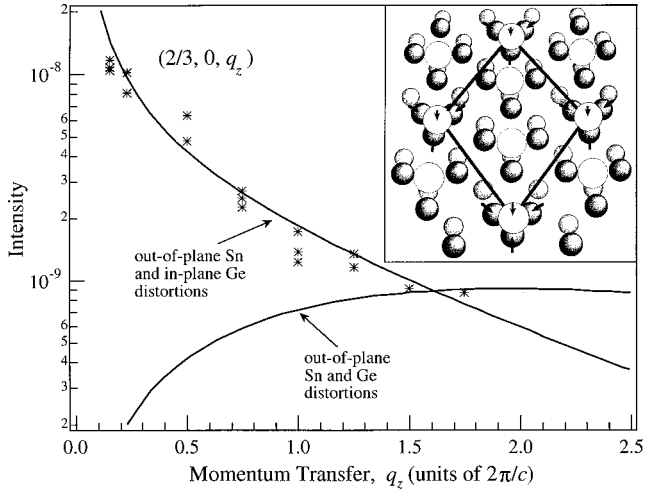

FIG. 3. Data from the $(\frac{2}{3},0)$ diffraction rod compared with two structural models. The lower line includes only vertical distortions of Sn and first layer Ge, while the upper line includes lateral displacements of the first layer Ge. A perspective view of the best-fit (3×3) structural model is shown in the inset, with arrows indicating displacements relative to the $(\sqrt{3}\times\sqrt{3})R30°$ structure. Displacements are exaggerated for clarity.

When the surface is cooled, one Sn atom per unit cell drops 0.04 Å closer to the Ge surface, and the three nearest Ge are drawn 0.22 Å further toward this Sn. Other atoms in the unit cell are to first order unchanged from the $(\sqrt{3}\times\sqrt{3})R30°$ structure. The Sn displacement is small and is dwarfed by the root-mean-squared (RMS) motion of the Sn; by far the most substantial atomic distortion occurs in the outermost Ge layer. We refer to this model as an ''inverted ripple'' since the inward displacement of the Sn ion cores is in the opposite direction from the valence charge observed in filled-state STM images.

The precise commensurability and the relatively large 0.22 Å Ge distortion present in this PLD each indicate the CDW originates from forces involving chemical bonding, that is a ''strong-coupling CDW.'' [11] Clearly the large corrugation (0.5 Å) in the valence electrons imaged with STM represents more than a structural change, since the Sn corrugation is small and of the opposite sign (-0.04 Å), and instead indicates a change in orbital occupancy. We can hypothesize as follows. Ge atoms on the clean (111) surface have one unpaired electron in an orbital oriented directly out from the surface due to sp^3 hybridization. These orbitals are not optimally oriented to bond to Sn in a $T4$ site; for Sn at a distance equal to the sum of the covalent radii of Sn and Ge ($1.40+1.22=2.62$ Å) the orbitals would need to be 62° off normal to be directed toward the Sn. A compromise is reached. In the room-temperature phase the Sn remains further from the surface, at a Sn-Ge distance of 2.95 Å, and the Ge move slightly in the surface plane toward the $T4$ site. As a result the Ge-Sn direction is only 50° away from normal. This is still far from optimal for either the Ge or Sn. At low temperatures, in the CDW phase, Ge atoms adjacent to one Sn atom per unit cell give up their effort to maintain bonding well-oriented toward substrate Ge atoms, i.e., give up their attempt at ideal sp^3 hybridization. Instead they are laterally displaced 0.22 Å further toward the Sn, and the Sn drops 0.04 Å toward the Ge, providing better bond overlap between Sn and Ge at the expense of Ge-Ge bonding. This reduces the Ge-Sn distance by 7.4%, to 2.70 Å, much closer to the sum of the covalent radii. The hybridization of Sn orbitals is of course modified also, and appears as contrast in STM images of the CDW phase. In this model, no charge transfer is required, instead the CDW represents orbital ordering. The actual driving force for this rehybridization must involve more than the simple chemical bonding described here. Electron correlation is important, otherwise the PLD would be the ground state in a local-density approximation calculation, contrary to calculations by Carpinelli *et al.*[6] Our measured PLD will set the standard by which new theories for the CDW can be evaluated.

Research at ORNL was sponsored by Department of Energy managed by Lockheed Martin Energy Research Corp. under Contract No. DF-AC05-96OR22464. E.W.P. and J.M.C. were supported by NSF DMR-9510132, and J.Z. was supported by NEDO (Japan).

[1] J. J. Métois and G. LeLay, Surf. Sci. **133**, 422 (1983); H. Huang, C. M. Wei, B. Tonner, and S. Y. Tong, Phys. Rev. Lett. **62**, 559 (1989); R. Feidenhans'l, J. S. Pedersen, M. Nielsen, F. Grey, and R. L. Johnson, *ibid.* **178**, 927 (1986); L. Seehofer, G. Falkenberg, and R. L. Johnson, *ibid.* **290**, 15 (1993).

[2] J. A. Carlisle, T. Miller, and T.-C. Chiang, Phys. Rev. B **47**, 3790 (1993); **47**, 10 342 (1993).

[3] T. Ichikawa and S. Ino, Surf. Sci. **105**, 395 (1981).

[4] J. S. Pedersen, R. Feidenhans'l, M. Nielsen, K. Kjaer, F. Grey, and R. L. Johnson, Surf. Sci. **189/190**, 1047 (1987).

[5] J. M. Carpinelli, H. H. Weitering, E. W. Plummer, and R. Stumpf, Nature (London) **381**, 398 (1996).

[6] J. M. Carpinelli, H. H. Weitering, M. Bartkowiak, R. Stumpf, and E. W. Plummer, Phys. Rev. Lett. **79**, 2859 (1997).

[7] J. Avila, A. Mascaraque, E. G. Michel, and M. C. Asensio (unpublished).

[8] A. Goldoni and S. Modesti, Phys. Rev. Lett. **79**, 3266 (1997).

[9] J. M. Carpinelli, Ph.D. thesis, University of Pennsylvania, 1997.

[10] I. K. Robinson and D. J. Tweet, Rep. Prog. Phys. **55**, 599 (1992); R. Feidenhans'l, Surf. Sci. Rep. **10**, 105 (1989).

[11] E. Tosatti, in *Electronic Surface and Interface States on Metallic Systems*, edited by E. Bertel and M. Donath (World Scientific, Singapore, 1995).

[12] D. Gibbs, B. M. Ocko, D. M. Zehner, and S. G. J. Mochrie, Phys. Rev. B **38**, 7303 (1988); A. R. Sandy, S. G. J. Mochrie, D. M. Zehner, K. G. Huang, and D. Gibbs, *ibid.* **43**, 4667 (1991).

[13] A. P. Baddorf, D. M. Zehner, G. Helgesen, D. Gibbs, A. R. Sandy, and S. G. J. Mochrie, Phys. Rev. B **48**, 9013 (1993).